

Research Article

Microemulsion Formulations for the Transdermal Delivery of Lapachol

Maria Alice Maciel Tabosa,¹ Ana Rosa Brissant de Andrade,¹ Ana Amélia Moreira Lira,²
Victor Hugo Vitorino Sarmiento,³ Davi Pereira de Santana,¹ and Leila Bastos Leal^{1,4}

Received 11 December 2017; accepted 12 March 2018; published online 10 April 2018

Abstract. This project was carried out to investigate the feasibility of using microemulsions for transdermal delivery of lapachol. From the screening of surfactants and oils, a range of microemulsions were developed using oleic acid, a mixture of Cremophor EL and Tween 20 and water. The solubility of lapachol was determined in these ingredients and in the formulated microemulsions. The microemulsions were characterised using cross-polarising light microscopy, their electrical conductivity, pH, zeta potential and rheology were analysed, and they were also investigated using small-angle X-ray scattering and differential scanning calorimetry. *Ex vivo* studies were performed using porcine ear skin and Franz diffusion cells to investigate the permeation and retention of lapachol. Systems containing different concentrations of Cremophor EL (8.4–41.6%), Tween 20 (5.4–41.6%) and oleic acid (12–31.9%) are able to form microemulsions. Lapachol was delivered more effectively through the skin from all of the microemulsions tested than by the control (oleic acid). These studies indicated that microemulsions incorporating lapachol were formed successfully and that these enhanced drug delivery and retention in the skin. Microemulsion systems may, therefore, provide promising vehicles for percutaneous delivery of lapachol.

KEY WORDS: controlled release; drug delivery systems; *in vitro* models; microemulsion; percutaneous; permeability; skin.

INTRODUCTION

Lapachol (2-hydroxy-3-(3-methylbut-2-enyl)naphthalene-1,4-dione) (Fig. 1) is an important naturally occurring naphthoquinone that was isolated from the bark of *Tabebuia avellanedae* (Mart. Ex DC.) Standl., in the mid-1950s by the industrial chemist, Oswaldo Gonçalves de Lima (1–3). It is a yellow powder that is weakly acidic (pKa = 6.15) and has a melting point between 139 and 142 °C (4).

Lapachol has been shown to have several pharmacological activities, including antimicrobial, antifungal, molluscicidal, leishmanicidal, trypanocidal, antimalarial, anti-inflammatory, anti-cancer, anti-ulcer, contraceptive and immunosuppressive effects (2,5–8). Its relatively low molecular weight (242 g mol⁻¹), moderate lipophilicity (log $P_{oil/water}$ = 2.69; water solubility = 2 mg L⁻¹ at 25 °C) and low oral bioavailability (9–11) are favourable factors for transdermal delivery. Therefore, topically applied lapachol could be suitable for systemic treatment of skin diseases.

Transdermal drug delivery has demonstrated the ability to enhance therapeutic efficacy, increase bioavailability and avoid adverse effects related to oral administration (12). However, the main challenge in the transdermal application is the barrier function of the skin, which is difficult for most drugs to overcome. Therefore, effective formulations capable of delivering therapeutic agents through this barrier are required (13). Different approaches have been employed to enhance drug skin permeation and bioavailability, including iontophoresis, sonophoresis, electroporation, microperforation of the *stratum corneum*, incorporation of penetration enhancers into the formulation, or solubilisation of the drug in a colloidal delivery system, such as microemulsions. This latter approach provides a promising alternative for transdermal delivery (14,15).

During recent decades, numerous studies have suggested that microemulsions have the potential to increase cutaneous

¹ Department of Pharmaceutical Science, Universidade Federal de Pernambuco, Avenida Professor Artur de Sá, s/n, Cidade Universitária, Recife, CEP 50740-521, Brazil.

² Department of Physiology, Universidade Federal de Sergipe, Cidade Universitária Professor Aloísio de Campos, Avenida Marechal Rondon s/n, Jardim Rosa Elze, São Cristóvão, CEP 49100-000, Brazil.

³ Department of Chemistry, Universidade Federal de Sergipe, Avenida Vereador Olímpio Grande, S/N, Campus Prof. Alberto Carvalho, Itabaiana, CEP 49500-000, Brazil.

⁴ To whom correspondence should be addressed. (e-mail: leila.leal@nudfac.com.br)

Abbreviations DSC, Differential scanning calorimetry; HLB, Hydrophilic-lipophilic balance; HPLC, High-performance liquid chromatography; PEG 400, Polyethylene glycol-400; SAXS, Small-angle X-ray scattering

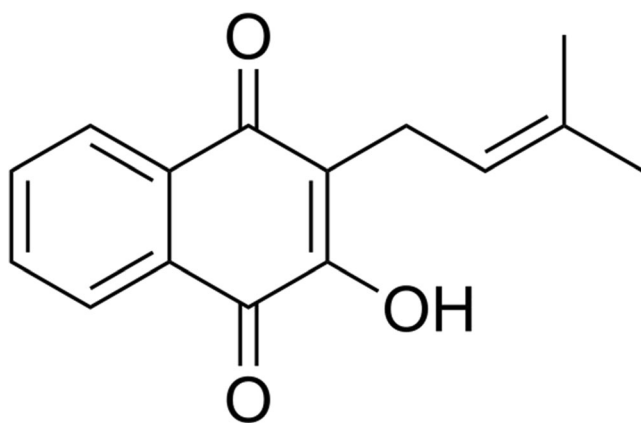


Fig. 1. Structure of lapachol

delivery of both hydrophilic and lipophilic drugs, as compared with conventional vehicles. A microemulsion is defined as a dispersion consisting of oil, surfactants and an aqueous phase; the droplets in these preparations are usually within the range of 10–100 nm. Microemulsions are typically optically isotropic, thermodynamically stable, and require no specific or sophisticated technology to produce (13,16,17).

In a previous work, our research group has demonstrated that lapachol has potential anti-inflammatory activity after topical application which was characterised by its ability to reduce the increase in hind-paw volume induced by carrageenan injection (10). However, to the author's knowledge, no attempt has previously been made to deliver lapachol via microsystems.

Therefore, the present study aimed to develop and characterise a transdermal microemulsion loaded with lapachol. To achieve this objective, pseudoternary phase diagrams were used as a tool to identify the microemulsion regions. Selected formulations were characterised by physicochemical properties and *ex vivo* skin permeation studies.

MATERIALS AND METHODS

Materials

Lapachol was obtained from the *Departamento de Antibiótico* at the *Universidade Federal de Pernambuco* (Recife, Brazil). Isopropyl myristate, polyethylene 20 sorbitan monolaurate (Tween 20®), polyethylene glycol-400 (PEG 400; VETEC, Brazil), polyglyceryl-6 dioleate (Plurol Oleique®; Gattefossé, France), polyoxy-35-castor oil (Cremophor EL®), sorbitane monooleate (Span 80®), oleic acid, olive oil (Sigma-Aldrich, Germany), *Orbignya oleifera* seed oil (Babaçu oil; Crodamazon Babaçu CO®), polyoxyethylene (18) oleyl ether (BRIJ™ O20; Croda, Spain) and methanol (high-performance liquid chromatography [HPLC] grade; JT Baker, USA) were obtained from the indicated suppliers. All aqueous solutions were prepared using high-purity deionised water with a conductance of $0.055 \mu\text{S cm}^{-1}$ ($18.2 \text{ M}\Omega \text{ cm}^{-1}$) (Purelab classic DI, Elga, UK).

Screening of Surfactants and Oils

The solubility of lapachol in a range of oils (isopropyl myristate, oleic acid, olive oil and Babaçu oil) and surfactants (Cremophor EL, Span 80, PEG 400 and Plurol Oleique) was

determined by vortex mixing excess lapachol with 5 mL of each oil or surfactant in stoppered vials (10 mL capacity) for 10 min. The vials were then kept at $25 \pm 1.0 \text{ }^\circ\text{C}$ in a Dubnoff shaker water bath with a thermostat (Q226M2; Quimis, Brazil) for 24 h to achieve equilibrium. The mixtures were then removed from the shaker and centrifuged at 3000 rpm (relative centrifugal force 754.65g) for 30 min to remove excess undissolved lapachol. The supernatants were filtered through a 0.45- μm cellulose acetate filter, and the drug concentration in the filtrate was determined using a UV spectrophotometer (Shimadzu UVmini-1249, Shimadzu, Japan) at a wavelength of 278 nm, after appropriate dilution (19).

Construction of Microemulsion Phase Diagrams

Based on the solubility studies, pseudoternary phase diagrams were constructed to obtain the concentration range of components for the existing microemulsion zones. Cremophor EL was blended with Tween 20 (S_{mix}) at weight ratios of 1:1, 1:5, 2:1, 5:1 and 7:3. Aqueous phase titration was used to construct the pseudoternary phase diagrams; this involved stepwise addition of distilled water to nine different ratios of oil and S_{mix} (1:9, 2:8, 3:7, 4:6, 5:5, 6:4, 7:3, 8:2 and 9:1 by weight) at $25 \text{ }^\circ\text{C}$ under magnetic stirring. After equilibration, the mixtures were assessed visually and categorised as either a one-phase microemulsion or a two-phase mixture. Turbidity was considered an indication of phase separation. Every sample that remained transparent and homogeneous after vigorous stirring was assigned to the monophasic area of the phase diagram. One axis of the pseudoternary phase diagram represented the aqueous phase, the other represented the oil phase and the third represented the S_{mix} (20).

Preparation of Lapachol Microemulsion

From each phase diagram constructed, different formulas were selected from the microemulsion region for incorporation of drug into the oil phase (oleic acid). Lapachol (0.5%) was dissolved gradually in oleic acid using magnetic stirring. After complete solubilisation, S_{mix} was added and the mixture was then diluted with water under moderate stirring.

Microemulsion Characterisation

Each formulation remained in equilibrium for 48 h for further characterisation. Formulations with and without drug were evaluated throughout this study.

Cross-Polarised Light Microscopy

A drop of each microemulsion sample was placed between a coverslip and a glass slide and observed using cross-polarised light microscopy (DM 750P; Leica Microsystems Heidelberg, Mannheim, Germany). In contrast to anisotropic liquid crystals, isotropic materials such as microemulsions will not interfere with polarised light (18) and the field of view remains dark. Photomicrographs were taken at $\times 20$ magnification.

Conductivity Measurements

Electrical conductivity was measured using a conductometer (CG 2200; GEHAKA, Brazil). The electrode was dipped in the microemulsion sample until the reading became stable. The conductivity cell constant was calibrated using standard KCl solutions. The measurements were performed in triplicate at 25 ± 1 °C.

pH Measurements

The pH of the selected oleic acid/S_{mix}/water microemulsions was measured using a pH meter (PG 1800; GEHAKA, Brazil). Triplicate measurements were performed.

Zeta Potential Measurements

Zeta potential distribution was measured with the ZetaSizer® Nano-ZS90 (Malvern Instruments, UK). Zeta limits ranged from -150 to 150 mV.

Rheological Analysis

The viscosity of the formulations was determined using a concentric cylinder rheometer (MCR-302®; Anton Paar, Austria). Shear rates of between 1 and 1000 s⁻¹ were used.

Small Angle X-Ray Scattering (SAXS)

The microemulsions were studied using small-angle X-ray scattering (SAXS). Measurements were performed at the Brazilian Synchrotron Light Laboratory (LNLS) using the SAXS synchrotron beamline. The incident X-ray monochromatic beam ($\lambda = 1.608$ Å) was monitored by means of a photomultiplier and detected on a Pilatus detector (8×8 binning). The SAXS chamber parasitic scattering was also registered (with bias and dark-noise subtraction) and subtracted from the sample pattern after sample attenuation correction. SAXS results were obtained from $I(q)$, as a function of the modulus of the scattering vector q , where $q = (4\pi/\lambda)\sin(\varepsilon/2)$ and ε represented the scattering angle. Each SAXS curve corresponds to a data collection time interval of 10 s.

Differential Scanning Calorimetry (DSC)

Differential scanning calorimetry (DSC) measurements were performed with a DSC-60 (Shimadzu, Japan) instrument equipped with a refrigerated cooling system (Peltier, EK90/SH, Germany). Nitrogen was used as the purge gas at a flow rate of 50 mL min⁻¹. Approximately 2–3 mg of sample was weighed precisely into hermetically sealable aluminium pans. An empty hermetically sealed pan was used as the reference. Measurements were carried out in cooling mode, where the sample was cooled from 25 °C to -50 °C at a rate of 10 °C min⁻¹. Sample thermograms were analysed using the TasyS® software (Shimadzu, Japan).

Solubility of Lapachol in the Microemulsion

Excess lapachol was vortex-mixed for 10 min with 5 mL of each microemulsion formulation in a 10-mL stoppered vial. The mixture vials were then kept at 25.0 ± 1.0 °C in a Dubnoff shaker water bath with a thermostat (Q226M2; Quimis, Brazil) for 24 h to achieve equilibrium. The mixtures were removed from the shaker and centrifuged at 3000 rpm (relative centrifugal force 754.65g) for 30 min to remove excess undissolved lapachol. The supernatants were filtered through a 0.45- μ m cellulose acetate filter. The filtrate was diluted with methanol and the lapachol concentration was determined using HPLC-UV, as described in the section below.

The saturation levels were calculated using the following equation, where C_v is the concentration of the drug dissolved in the vehicle and $C_{S,v}$ is the solubility of the drug in the vehicle (21).

$$\text{Saturation level (\%)} = \frac{C_v}{C_{S,v}}$$

HPLC-UV Assay of Lapachol

HPLC-UV analyses were performed using a Shimadzu HPLC system equipped with a UV detector, an autosampler and a reverse phase column (Phenomenex Gemini® Nx, 250 mm \times 4.6 mm, 5 μ m). A degassed 80:20 mixture of methanol and acetic acid aqueous solution (5%) was used to elute samples at ambient temperature at a flow rate of 1 mL min⁻¹; 20 μ L of each sample was injected. Samples and mobile phases were filtered through a 0.45- μ m cellulose acetate filter (Millipore, Bedford, MA), prior to HPLC analysis. UV detection was employed at a wavelength of 278 nm.

Ex vivo Skin Permeation and Distribution Studies

The skin permeation of lapachol from selected microemulsions was investigated *ex vivo* using porcine ear skin and a Franz diffusion cell with an effective diffusional area of 1.15 cm² and a receiver chamber capacity of 6 mL. Oleic acid with 0.5% lapachol was used as a control. The full thickness porcine skin was excised from the ear region, and hairs were removed using scissors. After preparation, the skin was stored at -20 °C prior to use (12). On the day of the experiment, the skin was brought to room temperature and mounted between the donor and receiver compartments of a Franz diffusion cell with the *stratum corneum* facing the donor compartment and the dermal side facing the receiver compartment. The donor compartment was initially empty, while the receiver chamber was filled with phosphate-buffer (pH 7.4) containing 3% BRIJ™ O20. The receiver fluid was stirred with a magnetic rotor at a speed of 300 rpm. The cells were equilibrated in a water bath at 37 ± 1 °C for 30 min; 300 mg of microemulsion formulation was then placed into the donor compartment. A 1-mL sample of the receptor fluid was collected at 2, 4, 6, 8, 12 and 24 h; this was immediately replaced by fresh solution. All samples were filtered through a 0.45- μ m cellulose acetate membrane and analysed for

lapachol by HPLC-UV. All experiments were performed in sextuplicate.

The cumulative amount of lapachol that permeated through the skin ($\mu\text{g cm}^{-2}$) was plotted as a function of time (t) for each formulation. The rate of drug permeation (J_{SS}) was determined from the slope of the linear portion of the cumulative drug permeation *versus* time plot. The permeability coefficient (K_p) was calculated by dividing J_{SS} by the initial concentration of drug in the donor cell (C_o), as shown by the following Equation (22):

$$K_p = J_{SS}/C_o$$

The enhancement ratio (ER) was calculated as the ratio of flux obtained with microemulsion formulations and control (oleic acid).

In order to determine the amount of lapachol accumulated by the skin (*stratum corneum* and viable epidermis/dermis) 24 h after sample application, the skin was removed, rinsed with distilled water and then carefully dried using absorbent paper. The *stratum corneum* was removed by tape-stripping; this involved the application and removal of 15 strips of adhesive tape (Durex™, 3 M, Brazil). Methanol (5 mL) was added to extract the tapes, mixed for 5 min, sonicated for 30 min and then filtered using a 0.45- μm cellulose acetate membrane (10). The resulting filtrate was assayed for lapachol by HPLC-UV. The remaining tissue was homogenised in 5 mL methanol, sonicated for 30 s, centrifuged and filtered prior to analysis of lapachol by HPLC-UV (10).

Data Analysis

All values are expressed as their mean \pm standard deviation. When comparing multiple groups, one-way or two-way analysis of variance (ANOVA) was applied with the Bonferroni multiple comparison procedures, with $p < 0.05$ as the minimum level of significance.

RESULTS

Screening of Surfactants and Oils

The solubility (mg mL^{-1}) of lapachol in a range of oils, as well as in different surfactants, is shown in Table I. The solubility of lapachol was found to be higher in oleic acid ($15.33 \pm 2.15 \text{ mg mL}^{-1}$) than in the other oils tested. Cremophor EL, Tween 20 and PEG 400 produced the greatest solubilisation of lapachol (30.39 ± 1.95 , 42.21 ± 3.11 and $29.48 \pm 2.23 \text{ mg mL}^{-1}$, respectively).

Construction of Microemulsion Phase Diagrams

In order to determine the appropriate concentration ranges for the microemulsion components, pseudoternary phase diagrams were constructed for different S_{mix} ratios, namely Cremophor EL/Tween 20 at various ratios. Comparison of these five pseudoternary phase diagrams (Fig. 2) showed that the largest microemulsion region was observed using Cremophor EL/Tween 20 at 5:1 *w/w*. The

Table I. Solubility of Lapachol in Oils and Surfactants at 25 ± 1 °C

Components	Solubility (mg mL^{-1}) ^a
Surfactants	
Cremophor EL	30.39 ± 1.95
Tween 20	42.21 ± 3.11
PEG 400	29.48 ± 2.23
Span 80	11.80 ± 1.15
Plurol Oleique	4.23 ± 0.86
Oils	
Isopropyl myristate	8.55 ± 1.04
Oleic acid	15.33 ± 2.35
Olive oil	6.63 ± 0.84
Babaçu oil	10.50 ± 1.64

^a Mean \pm standard deviation, $n = 3$

PEG 400 polyethylene glycol-400

microemulsion region expanded with a lower proportion of Tween 20 ($S_{\text{mix}}5:1$), while this region was smaller in the $S_{\text{mix}} 1:5$ phase diagram. Using this information, four formulations from the 5:1 S_{mix} pseudo-ternary phase diagram and one formulation from the $S_{\text{mix}} 1:5$ (ME 1–4 and ME 5, respectively, Table II) were selected for characterisation studies.

Microemulsion Characterisation

The physicochemical parameters of the loaded and unloaded microemulsions (ME1–5) are shown in Table III.

No birefringence was detected under the cross-polarised light microscope (not shown) for all drug-loaded formulations and their blanks counterparts. The electrical conductivity of the studied samples was relatively high (21.7 to $70.2 \mu\text{S cm}^{-1}$). The pH (4.1 to 4.9) and zeta potential values (-28.3 to -33.4 mV), in the presence or absence of lapachol, were similar.

All of the microemulsions tested exhibited a linear relationship between shear rate and shear stress (not shown). The viscosity values (0.68 to 14.74 Pa s^{-1}) tended to increase as the water concentration increased. Addition of lapachol caused a slight decrease in viscosity.

Figure 3 shows scattering intensity patterns, $I(q)$ in function of scattering vector (q) for both lapachol-loaded and unloaded microemulsions, where broad and wide peaks centred at different q -values are exhibited.

The thermal behaviour of water in these microemulsion systems was investigated by DSC and compared with that of pure doubled-distilled water, as shown in Fig. 4. Upon cooling, pure water showed an exothermic peak at approximately -22 °C. Similar peaks were observed in the ME 1 (35.6% water) and ME 3 (38.0% water) formulations at about -31 and -27 °C, respectively. However, water freezing was not observed in the ME 2, ME 4 or ME 5 formulations.

Solubility of Lapachol in Microemulsions

Table IV shows lapachol solubility and saturation level in each microemulsion. Although there were significant differences in lapachol solubility in the individual components (Table I), there were no significant differences in the

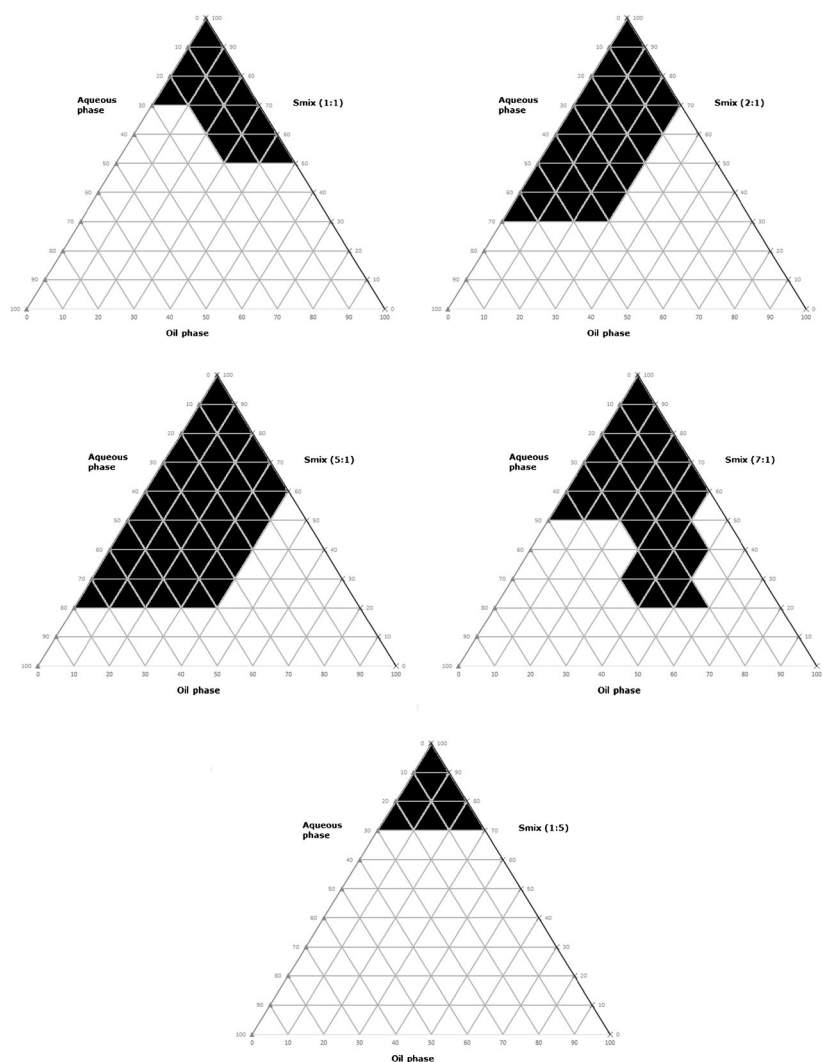


Fig. 2. Pseudoternary phase diagrams of the microemulsion region of oleic acid (oil phase), Cremophor EL and Tween 20 (surfactants in the S_{mix}), and water (aqueous phase) at different S_{mix} ratios

formulations (ME 1–4), except ME 5 which showed greater lapachol solubilisation.

Ex vivo Skin Permeation and Distribution Studies

Lapachol was delivered more effectively by the studied microemulsions than by oleic acid, as shown in Fig. 5. The values of a range of percutaneous parameters are presented in Table V. The permeation profiles followed Fick's diffusion law, with a steady time-dependent increase in the concentration of lapachol in the receiver. The microemulsions produced indistinguishable permeation rates at early time-points (≤ 6 h after sample application), although differences were evident at later time-points. Remarkably, ME1–4 delivered very similar cumulative amounts of lapachol, while ME 5 delivered significantly less lapachol. However, ME 5 did deliver significantly more lapachol than the oleic acid solution.

The results of the present study indicated that delivery using ME 1 produced greater skin accumulation of lapachol

in the epidermis+dermis than did delivery by the other MEs and the control. The values of K_p were higher for ME 3 and ME 4 than for other formulations. The enhancement ratios of the five microemulsions were 2.3–3.5-fold higher than that of the control.

Table II. Compositions of Selected Lapachol Microemulsion Formulations

Components	ME 1	ME 2	ME 3	ME 4	ME 5
Cremophor	27.1	41.6	41.6	28.75	8.4
Tween 20	5.4	8.4	8.4	5.75	41.6
Oleic Acid	31.9	24.5	12.0	12.0	24.5
Lapachol	0.16	0.12	0.06	0.06	0.12
Water	35.6	25.5	38	53.5	25.5

Data are provided as % (w/w)

Table III. Characteristics of Microemulsion Formulations

	Electrical conductivity ($\mu\text{S cm}^{-1}$) ^a		pH ^a		Zeta potential (mV) ^a		Viscosity (Pa s^{-1})	
	Unloaded	Loaded	Unloaded	Loaded	Unloaded	Loaded	Unloaded	Loaded
ME 1	60.4 \pm 0.2	41.9 \pm 0.1	4.6 \pm 0.1	4.2 \pm 0.1	-34.6 \pm 0.4	-30.3 \pm 0.5	6.95 \pm 1.43	5.91 \pm 1.67
ME 2	65.3 \pm 0.3	35.1 \pm 0.2	4.9 \pm 0.1	4.6 \pm 0.1	-28.8 \pm 0.4	-28.3 \pm 0.7	3.93 \pm 0.97	2.26 \pm 0.56
ME 3	53.0 \pm 0.2	41.2 \pm 0.1	4.5 \pm 0.1	4.1 \pm 0.1	-30.7 \pm 0.5	-31.1 \pm 0.4	8.98 \pm 1.17	6.60 \pm 1.65
ME 4	70.2 \pm 0.4	48.6 \pm 0.2	4.3 \pm 0.1	4.1 \pm 0.1	-29.7 \pm 0.4	-29.6 \pm 0.7	14.74 \pm 2.98	12.72 \pm 2.74
ME 5	52.6 \pm 0.1	21.7 \pm 0.1	4.9 \pm 0.1	4.4 \pm 0.1	-32.9 \pm 0.3	-33.4 \pm 0.4	0.71 \pm 0.22	0.68 \pm 0.29

^a Mean \pm standard deviation, $n = 3$

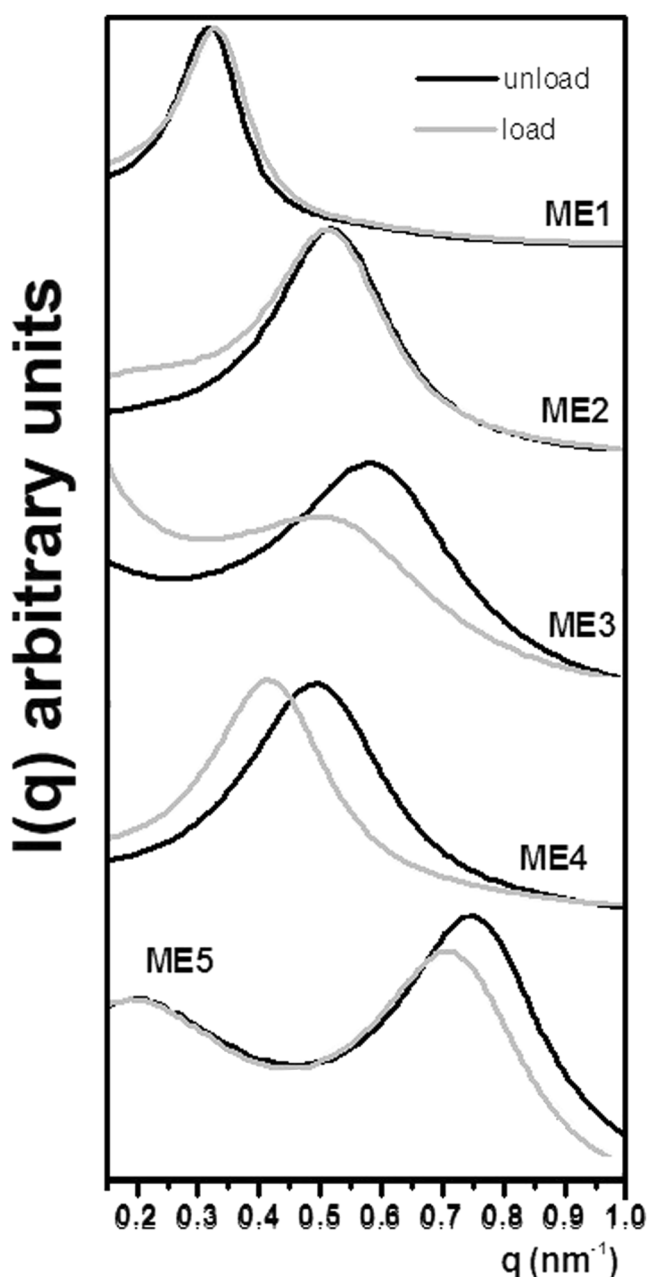


Fig. 3. Scattering intensity patterns $I(q)$ in function of scattering vector (q) for microemulsions (ME 1–5, as described in Table II) without (unloaded) and with (loaded) added lapachol

DISCUSSION

The physicochemical properties of the intended drug should be considered during the development of microemulsion formulations. Lipophilic drugs are encapsulated (mostly) in the oil phase of oil/water (o/w) microemulsions, whereas hydrophilic drugs are encapsulated (mostly) in the aqueous phase of w/o microemulsions. The solubility of lipophilic drugs in the oil phase and of hydrophilic drugs in the aqueous phase is, therefore, an important criterion informing the selection of these phases (12). Lapachol is a lipophilic drug and we, therefore, analysed its solubility in a range of oils, as well as in different surfactants (Table I). The solubility of lapachol was found to be higher in oleic acid ($15.33 \pm 2.15 \text{ mg mL}^{-1}$) than in the other oils tested. Oleic acid is considered to be non-irritating to the skin because it does not denature proteins (23). Moreover, it is widely used as a permeation enhancer, probably by destabilising skin lipids (24). Therefore, oleic acid was selected as the oil phase for the development of an optimised o/w microemulsion formulation for transdermal lapachol delivery.

The most critical problem in the development of microemulsion-based drug delivery systems is the toxicity of the surfactants. From the five nonionic surfactants tested in this work (Table I), three were selected for further analysis: Cremophor EL, Tween 20 and PEG 400, with hydrophilic-lipophilic balance (HLB) values of 14.0, 11.6 and 16.7, respectively. The surfactant HLB value is important because low-HLB surfactants are favoured for the formulation of w/o microemulsions, whereas high-HLB surfactants (such as those chosen in this study) are preferred for the formation of o/w microemulsions (25,26). As Cremophor EL and Tween 20 solubilised the most lapachol, they were selected for the development of a suitable o/w microemulsion.

It is known that large amounts of surfactant may cause skin irritation. It is therefore important to determine the surfactant concentration properly and to use the minimum concentration required for the development of the microemulsion formulation (12). The surfactants chosen in this work are generally regarded as having low toxicity and skin irritancy and, therefore, considered to be acceptable for transdermal administration.

Surfactants present in the microemulsions may cause increased membrane fluidity by solubilisation or extraction of lipids present in the *stratum corneum* and alter tight junction properties (27), leading to increased permeation. However, it

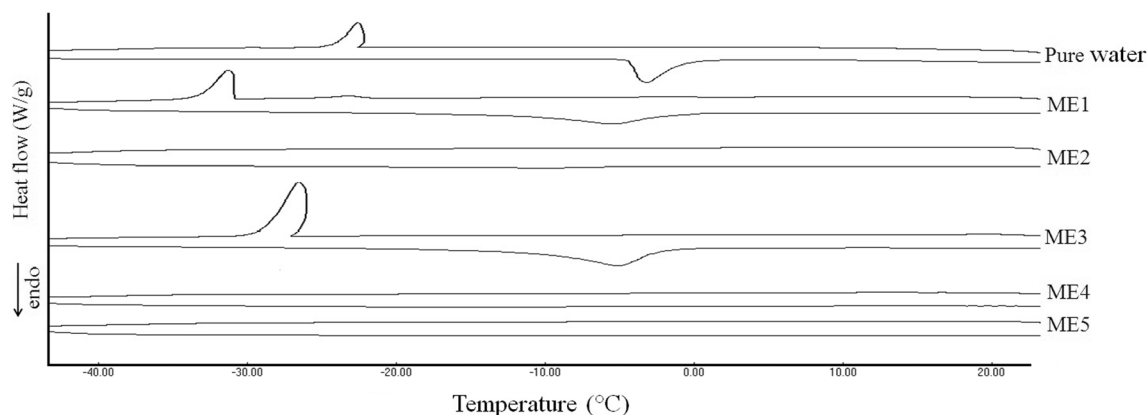


Fig. 4. Differential scanning calorimetry (DSC) cooling curves (plotted as exothermic heat flow as a function of temperature) of pure water and of the indicated microemulsions (ME 1–5, as described in Table II)

is widely accepted that the type of microemulsion employed is also an important determinant of drug delivery, because its internal structure, composition, droplet size and viscosity can influence the process of drug release (28).

All the formulations were prepared with and without lapachol and remained clear and without the presence of sediments. Examination of those formulations using cross-polarised light microscopy (not shown) presented no birefringence; this indicated that they showed the same optical properties in all directions, as would be expected from microemulsions (29). Incorporation of lapachol into those systems did not change their isotropic behaviour, confirming the continuity of the microemulsion system.

Electrical conductivity measurements confirmed that we had generated o/w microemulsions, which have relatively high electrical conductivity ($\sim 10\text{--}100 \mu\text{S cm}^{-1}$), and not w/o microemulsions, where electrical conductivity tends to be $< 10 \mu\text{S cm}^{-1}$ (30). The electrical conductivity of the loaded microemulsions ($21.7\text{--}65.3 \mu\text{S cm}^{-1}$) reflected the acidity of lapachol, which has a pKa of 6.15 (31). When dispersed in a medium with a pH that is lower than its pKa, it tends to remain in the unionised form and interacts with the aqueous phase; this reduces the electrical conductivity, as can be seen in the data in Table III.

The pH of the microemulsions ranged from 4.1 to 4.9 (Table III). A higher water content increases the ionisation of oleic acid; this releases more protons into the solution and thereby reduces the pH (28). It is evident from Table III that all of the microemulsion systems were within the acceptable physiologic pH range for dermal preparations (pH 4.0–7.0) (32). Measurement of zeta potential provides information about the surface charge properties and the long-term physical stability of the microemulsions (33). The zeta potential required for purely electrostatic stabilisation of colloidal particles is typically $\pm 25\text{--}30 \text{ mV}$ (34). The zeta potential values of these formulations (-28.3 to -33.4 mV) suggested that all systems are physically stable.

The viscosity of a microemulsion is determined by the levels and types of surfactant(s), oil(s) and water present (28). All of the microemulsions tested exhibited a linear relationship between shear rate and shear stress (not shown), indicating the Newtonian fluid properties of microemulsions (14,35). The viscosity values tended to increase as the water

concentration increased. This might reflect interactions between the microemulsion droplets in these o/w systems. It has been found that the hydrophilic chains of non-ionic surfactants are expected to be strongly hydrated and connected *via* hydrogen bonds, allowing interaction between the droplets (36–38). The addition of lapachol caused a slight decrease in viscosity (Table III). This may reflect an inhibition of strong attractive forces (39) by lapachol, due to its lipophilic nature.

Characteristic microemulsion curves were obtained from the SAXS scatterings, which confirm the results of cross-polarised light microscopy. We can also observe that the maximum of the peaks are shifted to higher q -values as the surfactants amount increases (Cremophor and Tween blended). From the relationship $q = 2\pi/d$, this increase in the q -values is due to decrease of distance d between scattering objects domains attributed to differences in the scattering length density (SLD) between polar and apolar domains (droplet size) of microemulsions, in the case of this study. With increasing surfactant blend content, the position of the peaks shifts toward larger q -values indicating a decrease in the droplet size. These results are consistent since surfactants used in the preparation of the microemulsions reduced the interfacial tension and consequently droplet size. Other authors (40,41) have reported similar findings in relation to the microstructural properties of non-ionic microemulsions. The addition of lapachol promotes the increase of droplet size since a shift toward lower q -values is observed. This behaviour is enhanced for ME 3, ME 4 and ME 5 probably

Table IV. Solubility of Lapachol in the Microemulsions at $25 \pm 1 \text{ }^\circ\text{C}$

Formulation	Concentration of the drug dissolved in the formulation (mg mL^{-1})	Solubility of the drug in the formulation (mg mL^{-1}) ^a	Saturation level (%) ^a
ME 1	1.6	8.11 ± 2.35	19.94 ± 2.56
ME 2	1.2	7.10 ± 0.41	16.94 ± 0.98
ME 3	0.6	6.55 ± 0.41	9.19 ± 0.60
ME 4	0.6	6.53 ± 0.49	9.22 ± 0.71
ME 5	1.2	13.95 ± 5.63	9.55 ± 3.60

^a Mean \pm standard deviation, $n = 3$

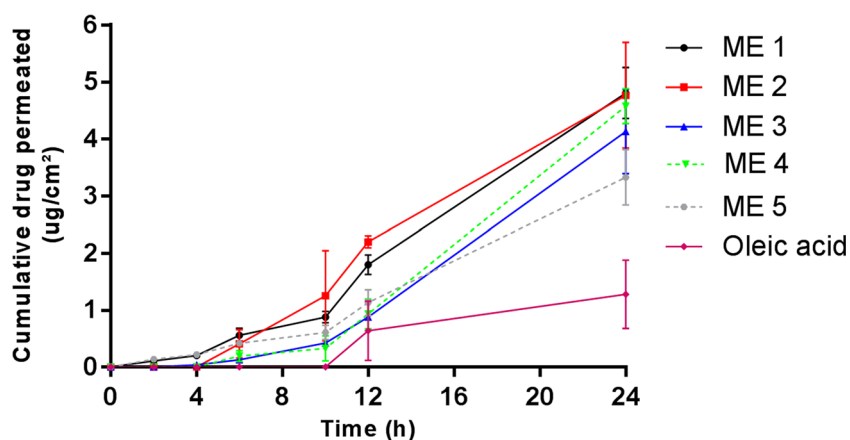


Fig. 5. *Ex vivo* skin permeation profile of lapachol delivered using the indicated microemulsions (ME1–5, as described in Table II) or oleic acid solution

due to the increased volume of the oily internal phase by lapachol which is lipophilic.

Investigating the thermal behaviour of water provides a rapid approach to understanding the microstructure of microemulsions (13). The water can be either bound or free, depending on its state within the microemulsion system, and DSC detects the resultant differences in its melting point and freezing behaviour (38).

The exothermic peak at approximately $-22\text{ }^{\circ}\text{C}$ showed in the pure water indicates its freezing point in the absence of any interactions with other molecules (42). Comparable peaks were observed in the ME 1 and ME 3 (at -31 and $-27\text{ }^{\circ}\text{C}$, respectively). However, the reduced freezing temperatures (as compared to pure water) show some interactions with other molecules (partial miscibility of water and surfactants). Interestingly, water freezing was not observed in the ME 2, ME 3 or ME 5 formulations. Those microemulsions contained less water and more surfactant, leading to more strongly bound water molecules being required to hydrate the polar head groups (14).

Although there were significant differences in lapachol solubility in the individual components (Table I), there were no significant differences in lapachol solubility in ME 1, 2, 4 and 3. ME 5 showed greater lapachol solubilisation, indicating that the proportion of S_{mix} had more influence than the microemulsion structure (43). ME 1 and ME 2 showed a

greater saturation level when compared with the other formulations; that said, we would expect that these two formulations (1 and 2) would show a greater permeation due to the higher thermodynamic activity.

In this *ex vivo* system, lapachol was delivered more effectively by these microemulsions than by oleic acid, as shown in Fig. 5. Although oleic acid is widely used as a penetration enhancer in topical dermatological preparations, either alone or in combination with other penetration enhancers (44), the microemulsion systems showed better performance in this study.

The cumulative amount of lapachol that permeated through the skin from all of the microemulsions tested was significantly greater than the amount delivered by the control, indicating that the permeation of lapachol was markedly influenced by these formulations. In addition, the enhancement ratios demonstrate that microemulsions can potently enhance transdermal delivery. Amongst the five microemulsion formulations investigated in this work, ME 5 had the lowest amount of lapachol permeated. As can be seen in Table IV, lapachol had a greater solubility in ME 5. In general, saturated solutions show the highest thermodynamic activity, which is well-known as a driving force for drug release and penetration into the skin (33). However, the saturation level of the ME 5 was similar to ME 3 and ME 4 showing that this was not the predominant parameter in the skin permeation of the drug.

Table V. Microemulsion Permeability Parameters

	ME 1	ME 2	ME 3	ME 4	ME 5	Oleic acid
Q_{24} ($\mu\text{g cm}^{-2}$) ^a	4.71 ± 0.44^b	4.87 ± 0.72^b	4.58 ± 0.30^b	4.13 ± 0.54^b	3.83 ± 0.48^b	1.27 ± 0.60
Enhancement ratio	3.3	3.5	2.8	3.2	2.3	–
J_{ss} ($\mu\text{g cm}^{-2} \text{h}^{-1}$) ^a	0.20 ± 0.05^b	0.21 ± 0.05^b	0.17 ± 0.07^b	0.19 ± 0.08^b	0.14 ± 0.03	0.06 ± 0.03
K_p (cm h^{-1}) ^a $\times 10^{-5}$	12.79 ± 3.38	17.77 ± 3.83^b	28.85 ± 12.02^b	31.83 ± 14.08^b	11.55 ± 3.24	1.13 ± 0.54
Q_{SC} ($\mu\text{g cm}^{-2}$) ^a	1.60 ± 0.36	1.77 ± 0.41	1.58 ± 0.54	1.80 ± 0.54	1.01 ± 0.07	1.08 ± 0.39
Q_{ED} ($\mu\text{g cm}^{-2}$) ^a	5.35 ± 1.29^b	4.62 ± 1.61	2.36 ± 0.52	3.13 ± 1.17	2.08 ± 0.69	3.17 ± 0.46

^a Mean \pm standard deviation, $n = 6$

^b $p < 0.05$, when compared with control (oleic acid)

Q_{24} cumulative amount of lapachol that had permeated through the skin, 24 h after sample application; J_{ss} rate of drug permeation; K_p permeability coefficient; Q_{SC} amount of lapachol accumulated in the *stratum corneum*, 24 h after sample application; Q_{ED} amount of lapachol accumulated in the viable epidermis + dermis, 24 h after sample application

The results of the present study indicated that, even though ME 1 has the lowest surfactant concentration, it has produced greater skin (epidermis+dermis) accumulation of lapachol than did delivery using the other formulations. As dermis is a hydrophilic layer irrigated by the blood circulation, any substance reaching it can pass into the systemic circulation. The lack of blood flow in *ex vivo* experiments means that the dermis creates a barrier to diffusion for these compounds that might not exist in the native *in vivo* setting. Therefore, during permeation studies, it is important to also take into account the amount of drug which stays accumulated in the dermis compartment. This information may shed light on the more realistic amount of drug which would reach the blood circulation *in vivo*.

The values of J_{ss} were higher for ME 1, ME 2 and ME 5 than for ME 3 and ME 4. High J_{ss} can create higher drug concentration within the upper layers of the skin and may also reflect the entry of formulation components into the bloodstream through the skin as penetration enhancers. In each formulation, all components could act as penetration enhancers with different mechanisms of action (13).

On the other hand, the values of K_p were higher for ME 3 and ME 4. Formulation 5 presented the lowest permeation performance amongst the microemulsions tested. The solubility of the drug in the formulation and proportion of the surfactant seems to have influenced the formulations directly and proportionately. However, saturation level and viscosity showed not to effect the permeation parameters of the drug. ME 5 that showed the lowest viscosity and highest solubility of the drug in the formulation presented lower Q_{24} and K_p . In general, the lower the viscosity, the greater the release of drug.

CONCLUSION

This study showed that systems containing Cremophor EL, Tween 20, oleic acid and water were able to form microemulsions. ME 1 presented lowest surfactant concentrations and high J_{ss} and epidermis+dermis accumulation, and this formulation showed to be the best transdermal formulation amongst the formulations tested. Further work is required to determine whether this formulation is clinically effective while minimising skin irritation.

ACKNOWLEDGEMENTS

The authors thank the Laboratório Nacional de Luz Síncrotron (LNLS, Campinas SP, Brazil). LNLS is acknowledged through the projects D11A-SAXS1-14558. We especially thank SAXS staff for the support. The authors also thank FECDA/NUDFAC for financial support.

REFERENCES

- Hussain H, Krohn K, Ahmad VU, Miana GA, Green IR. Lapachol: an overview. *ARKIVOC*. 2007;2:145–71.
- Almeida ERD. Preclinical and clinical studies of lapachol and beta-lapachone. *Open Nat Prod J*. 2009;2(1):42–7.
- Ferreira SB, Gonzaga DTG, Santos WC, Araújo KG, Ferreira VF. beta-Lapachona: Sua Importância em Química Medicinal e Modificações Estruturais. *Rev Virtual Quím*. 2010;2(2):140–60.
- Tabosa MAM, de Melo EKS, de Souza Dantas IMF, de Santana DP, Leal LB. Physicochemical characterization of lapachol. *Afr J Pharm Pharmacol*. 2015;9(5):131–8.
- de Almeida ER, da Silva Filho AA, Dos Santos ER, Lopes CAC. Antiinflammatory action of lapachol. *J Ethnopharmacol*. 1990;29(2):239–41.
- Guerra MO, Mazoni A, Brandão M, Peters V. Toxicology of lapachol in rats: embryolethality. *Rev Bras Biol*. 2001;61(1):171–4.
- de Andrade-Neto VF, Goulart MO, da Silva Filho JF, da Silva MJ, Pinto Mdo C, Pinto AV, et al. Antimalarial activity of phenazines from lapachol, beta-lapachone and its derivatives against *Plasmodium falciparum in vitro* and *Plasmodium berghei in vivo*. *Bioorg Med Chem Lett*. 2004;14(5):1145–9. <https://doi.org/10.1016/j.bmcl.2003.12.069>.
- Peres RS, Santos GB, Cecilio NT, Jabor VA, Niehues M, Torres BG, et al. Lapachol, a compound targeting pyrimidine metabolism, ameliorates experimental autoimmune arthritis. *Arthritis Res Ther*. 2017;19(1):47.
- Pisani DE, Elliot AJ, Hinman DR, Aaronson LM, Pardini RS. Relationship between inhibition of mitochondrial respiration by naphthoquinones, their antitumor activity, and their redox potential. *Biochem Pharmacol*. 1986;35(21):3791–8.
- Lira AA, Sester EA, Carvalho AL, Strattmann RR, Albuquerque MM, Wanderley AG, et al. Development of lapachol topical formulation: anti-inflammatory study of a selected formulation. *AAPS PharmSciTech*. 2008;9(1):163–8. <https://doi.org/10.1208/s12249-007-9002-z>.
- Lima NM, Correia CS, Leon LL, Machado G, Madeira MF, Santana AEG, et al. Antileishmanial activity of lapachol analogues. *Mem Inst Oswaldo Cruz*. 2004;99(7):757–61.
- Shakeel F, Ramadan W. Transdermal delivery of anticancer drug caffeine from water-in-oil nanoemulsions. *Colloids Surf B: Biointerfaces*. 2010;75(1):356–62. <https://doi.org/10.1016/j.colsurfb.2009.09.010>.
- Chaiyana W, Rades T, Okonogi S. Characterization and *in vitro* permeation study of microemulsions and liquid crystalline systems containing the anticholinesterase alkaloidal extract from *Tabernaemontana divaricata*. *Int J Pharm*. 2013;452(1–2):201–10. <https://doi.org/10.1016/j.ijpharm.2013.05.005>.
- Hathout RM, Woodman TJ, Mansour S, Mortada ND, Geneidi AS, Guy RH. Microemulsion formulations for the transdermal delivery of testosterone. *Eur J Pharm Sci*. 2010;40(3):188–96. <https://doi.org/10.1016/j.ejps.2010.03.008>.
- Fouad SA, Basalious EB, El-Nabarawi MA, Tayel SA. Microemulsion and poloxamer microemulsion-based gel for sustained transdermal delivery of diclofenac epolamine using in-skin drug depot: *in vitro/in vivo* evaluation. *Int J Pharm*. 2013;453(2):569–78. <https://doi.org/10.1016/j.ijpharm.2013.06.009>.
- Zhao JH, Ji L, Wang H, Chen ZQ, Zhang YT, Liu Y, et al. Microemulsion-based novel transdermal delivery system of tetramethylpyrazine: preparation and evaluation *in vitro* and *in vivo*. *Int J Nanomedicine*. 2011;6:1611–9. <https://doi.org/10.2147/IJN.S23597>.
- Nikumbh KV, Sevankar SG, Patil MP. Formulation development, *in vitro* and *in vivo* evaluation of microemulsion-based gel loaded with ketoprofen. *Drug Delivery*. 2015;22(4):509–215. <https://doi.org/10.3109/10717544.2013.859186>.
- Friberg SE. Micelles, microemulsions, liquid crystals, and the structure of stratum corneum lipids. *J Soc Cosmet Chem*. 1990;41(3):155–71.
- Yu A, Wang H, Wang J, Cao F, Gao Y, Cui J, et al. Formulation optimization and bioavailability after oral and nasal administration in rabbits of puerarin-loaded microemulsion. *J Pharm Sci*. 2011;100(3):933–41. <https://doi.org/10.1002/jps.22333>.
- Hosny KM, Hassan AH. Intranasal in situ gel loaded with saquinavir mesylate nanosized microemulsion: preparation, characterization, and *in vivo* evaluation. *Int J Pharm*. 2014;475(1–2):191–7. <https://doi.org/10.1016/j.ijpharm.2014.08.064>.
- Moser K, Kriwet K, Naik A, Kalia YN, Guy RH. Passive skin penetration enhancement and its quantification *in vitro*. *Eur J Pharm Biopharm*. 2001;52(2):103–12.
- Azeem A, Ahmad FJ, Khar RK, Talegaonkar S. Nanocarrier for the transdermal delivery of an antiparkinsonian drug. *AAPS PharmSciTech*. 2009;10(4):1093–103.
- Boelsma E, Tanojo H, Boddé H, Ponec M. Assessment of the potential irritancy of oleic acid on human skin: evaluation *in vitro* and *in vivo*. *Toxicol in Vitro*. 1996;10(6):729–42.

24. Martins M, Veiga F. Promotores de permeação para a liberação transdérmica de fármacos: uma nova aplicação para as ciclodextrinas. *Braz J Pharm Sci.* 2002;38(1):33–54.
25. Talegaonkar S, Azeem A, Ahmad FJ, Khar RK, Pathan SA, Khan ZI. Microemulsions: a novel approach to enhanced drug delivery. *Recent Pat Drug Deliv Formul.* 2008;2(3):238–57.
26. Moghassemi S, Hadjizadeh A. Nano-niosomes as nanoscale drug delivery systems: an illustrated review. *J Control Release.* 2014;185:22–36.
27. Rege BD, Kao JP, Polli JE. Effects of nonionic surfactants on membrane transporters in Caco-2 cell monolayers. *Eur J Pharm Sci.* 2002;16(4):237–46.
28. Bhatia G, Zhou Y, Banga AK. Adapalene microemulsion for transfollicular drug delivery. *J Pharm Sci.* 2013;102(8):2622–31. <https://doi.org/10.1002/jps.23627>.
29. Patel HK, Barot BS, Parejiya PB, Shelat PK, Shukla A. Topical delivery of clobetasol propionate loaded microemulsion based gel for effective treatment of vitiligo: ex vivo permeation and skin irritation studies. *Colloids Surf B: Biointerfaces.* 2013;102:86–94. <https://doi.org/10.1016/j.colsurfb.2012.08.011>.
30. Baroli B, López-Quintela MA, Delgado-Charro MB, Fadda AM, Blanco-Méndez J. Microemulsions for topical delivery of 8-methoxsalen. *J Control Release.* 2000;69(1):209–18.
31. Epifano F, Genovese S, Fiorito S, Mathieu V, Kiss R. Lapachol and its congeners as anticancer agents: a review. *Phytochem Rev.* 2013;13(1):37–49. <https://doi.org/10.1007/s11101-013-9289-1>.
32. Hashem FM, Shaker DS, Ghorab MK, Nasr M, Ismail A. Formulation, characterization, and clinical evaluation of microemulsion containing clotrimazole for topical delivery. *AAPS PharmSciTech.* 2011;12(3):879–86. <https://doi.org/10.1208/s12249-011-9653-7>.
33. Chen Y, Liu J, Yang X, Zhao X, Xu H. Oleanolic acid nanosuspensions: preparation, in-vitro characterization and enhanced hepatoprotective effect. *J Pharm Pharmacol.* 2005;57(2):259–64. <https://doi.org/10.1211/0022357055407>.
34. Meagher MJ, Leone B, Turnbull TL, Ross RD, Zhang Z, Roeder RK. Dextran-encapsulated barium sulfate nanoparticles prepared for aqueous dispersion as an X-ray contrast agent. *J Nanopart Res.* 2013;15:1246. <https://doi.org/10.1007/s11051-013-2146-8>.
35. Ge S, Lin Y, Lu H, Li Q, He J, Chen B, et al. Percutaneous delivery of econazole using microemulsion as vehicle: formulation, evaluation and vesicle-skin interaction. *Int J Pharm.* 2014;465(1–2):120–31. <https://doi.org/10.1016/j.ijpharm.2014.02.012>.
36. Podlogar F, Gasperlin M, Tomsic M, Jamnik A, Rogac MB. Structural characterisation of water-Tween 40/Imwitor 308-isopropyl myristate microemulsions using different experimental methods. *Int J Pharm.* 2004;276(1–2):115–28. <https://doi.org/10.1016/j.ijpharm.2004.02.018>.
37. Mitra RK, Paul BK. Physicochemical investigations of microemulsification of eucalyptus oil and water using mixed surfactants (AOT+ Brij-35) and butanol. *J Colloid Interface Sci.* 2005;283(2):565–77.
38. Boonme P, Krauel K, Graf A, Rades T, Junyaprasert VB. Characterization of microemulsion structures in the pseudoternary phase diagram of isopropyl palmitate/water/Brij 97: 1-butanol. *AAPS PharmSciTech.* 2006;7(2):E99–E104.
39. Podlogar F, Bester Rogac M, Gasperlin M. The effect of internal structure of selected water-Tween 40-Imwitor 308-IPM microemulsions on ketoprofene release. *Int J Pharm.* 2005;302(1–2):68–77. <https://doi.org/10.1016/j.ijpharm.2005.06.023>.
40. Mouri A, Diat O, El Ghzaoui A, Bauer C, Maurel JC, Devoisselle JM, et al. Phase behavior of reverse microemulsions based on Peceol((R)). *J Colloid Interface Sci.* 2014;416:139–46. <https://doi.org/10.1016/j.jcis.2013.10.058>.
41. Regev O, Ezrahi S, Aserin A, Garti N, Wachtel E, Kaler E, et al. A study of the microstructure of a four-component nonionic microemulsion by cryo-TEM, NMR, SAXS, and SANS. *Langmuir.* 1996;12(3):668–74.
42. Sintov AC, Greenberg I. Comparative percutaneous permeation study using caffeine-loaded microemulsion showing low reliability of the frozen/thawed skin models. *Int J Pharm.* 2014;471(1):516–24.
43. Peltola S, Saarinen-Savolainen P, Kiesvaara J, Suhonen TM, Urtti A. Microemulsions for topical delivery of estradiol. *Int J Pharm.* 2003;254(2):99–107. [https://doi.org/10.1016/s0378-5173\(02\)00632-4](https://doi.org/10.1016/s0378-5173(02)00632-4).
44. Lane ME. Skin penetration enhancers. *Int J Pharm.* 2013;447(1–2):12–21. <https://doi.org/10.1016/j.ijpharm.2013.02.040>.